Supplementary Materials

Phosphate-tolerant PtCo alloys enabled by sulfur-doped carbon encapsulation for ultra-low-Pt-loading HT-PEMFCs

Zhuofan Gan[1], Zhixu Chen[2], Peixi Qiu[1], Jingwen Cao[1], Jiangyun Bai[1], Feng Ji[3], Zhongxin Chen[4,*], Chengwei Deng[3,*], Chengyong Shu[1,*], Wei Tang[1,*]

[1]School of Chemical Engineering and Technology, Xi'an Jiaotong University, Xi'an 710049, Shaanxi, China.
[2]National Innovation Platform (Center) for Industry-Education Integration of Energy Storage Technology, Xi'an Jiaotong University, Xi'an 710049, Shaanxi, China.
[3]State Key Laboratory of Space Power-Sources Technology, Shanghai Institute of Space Power-Sources, Shanghai 200245, China.
[4]School of Science and Engineering, The Chinese University of Hong Kong, Shenzhen 518172, Guangdong, China.

***Correspondence to:** Prof. Wei Tang, School of Chemical Engineering and Technology, Xi'an Jiaotong University, No. 28, Xianning West Road, Xi'an 710049, Shaanxi, China. E-mail: tangw2018@mail.xjtu.edu.cn; Prof. Chengyong Shu, School of Chemical Engineering and Technology, Xi'an Jiaotong University, No. 28, Xianning West Road, Xi'an 710049, Shaanxi, China. E-mail: kowscy-n@mail.xjtu.edu.cn; Dr. Chengwei Deng, State Key Laboratory of Space Power-Sources Technology, Shanghai Institute of Space Power-Sources, No. 2965, Dongchuan Road, Shanghai 200245, China. E-mail: dengchengwei@spacechina.com; Prof. Zhongxin Chen, School of Science and Engineering, The Chinese University of Hong Kong, No. 2001, Longxiang Avenue, Shenzhen 518172, Guangdong, China. E-mail: chenzhongxin@cuhk.edu.cn

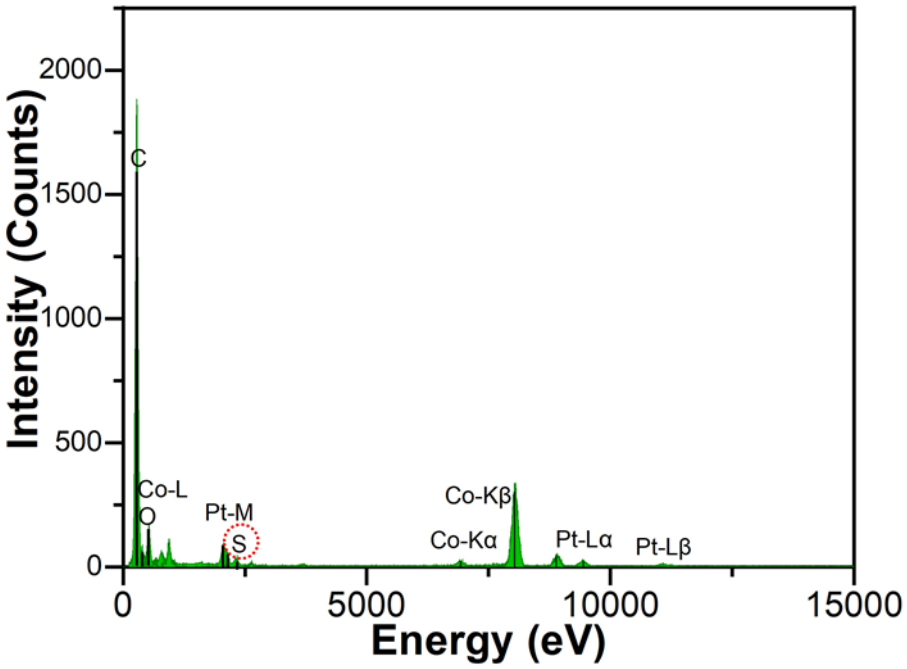

Supplementary Figure 1. EDS spectra of STG-PtCo/EC sample.

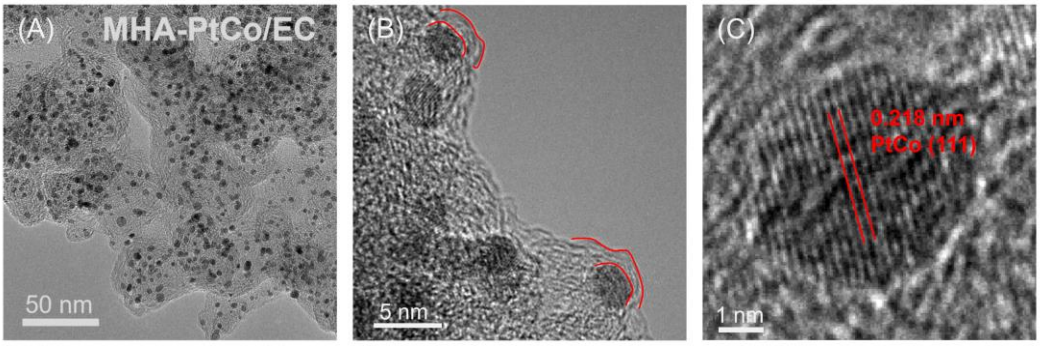

Supplementary Figure 2. (A,B) TEM images and (C) HR-TEM image of MHA-PtCo/EC.

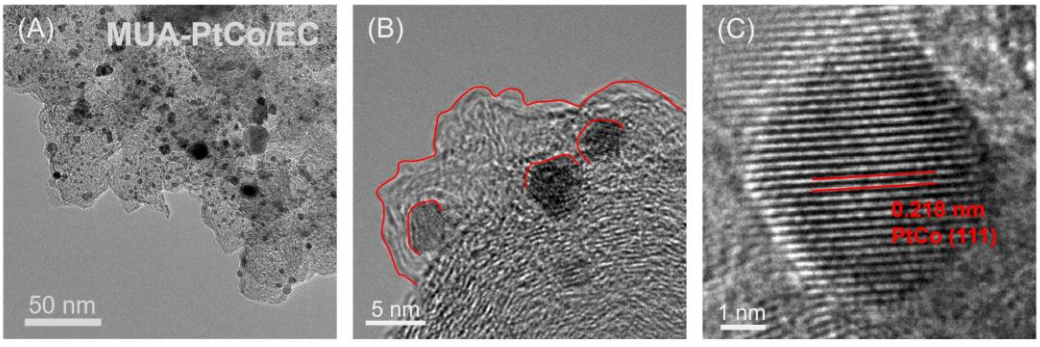

Supplementary Figure 3. (A,B) TEM images and (C) HR-TEM image of MUA-PtCo/EC.

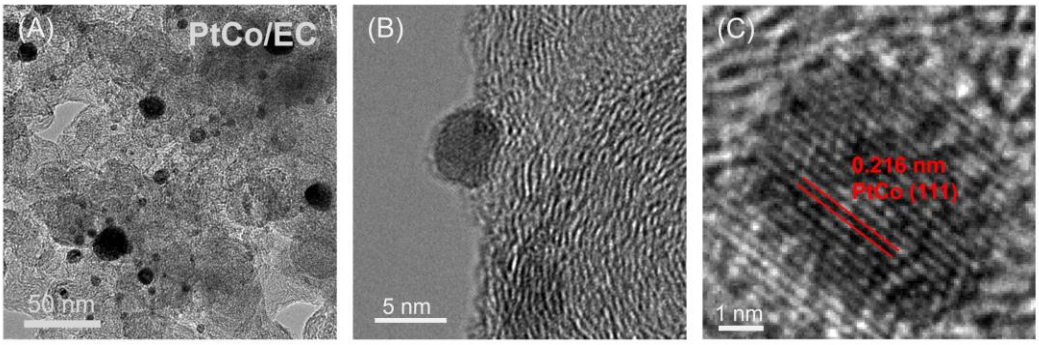

Supplementary Figure 4. (A,B) TEM images and (C) HR-TEM image of PtCo/EC.

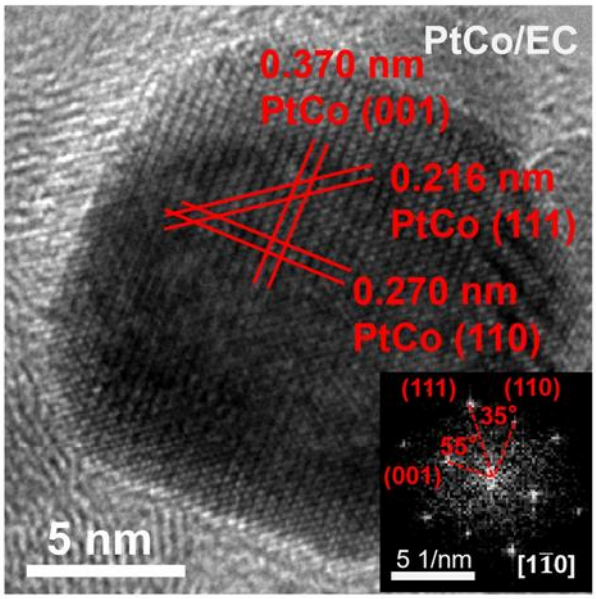

Supplementary Figure 5. HR-TEM image of PtCo/EC sample.

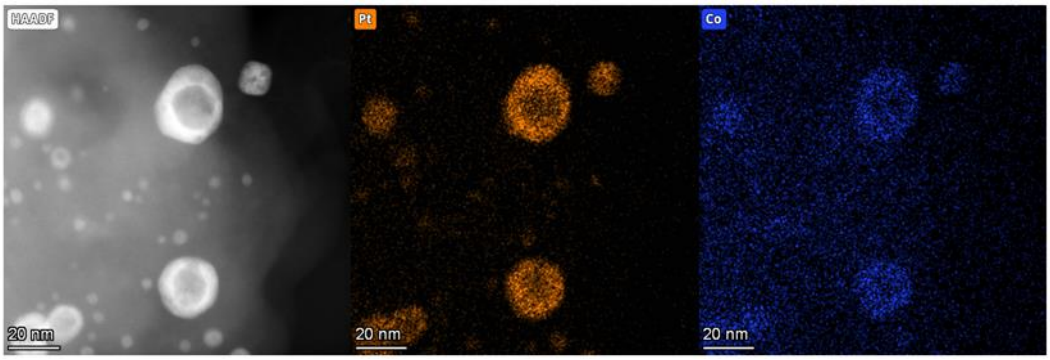

Supplementary Figure 6. HAADF-STEM image and EDS mapping of PtCo/EC sample.

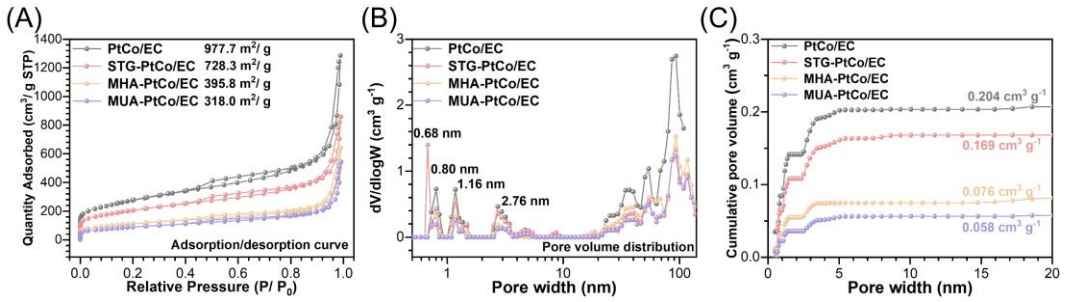

Supplementary Figure 7. (A) Nitrogen ad-/de-sorption isotherms, (B) pore volume distribution and (C) cumulative pore volume distribution of small-molecule-assisted PtCo/EC samples.

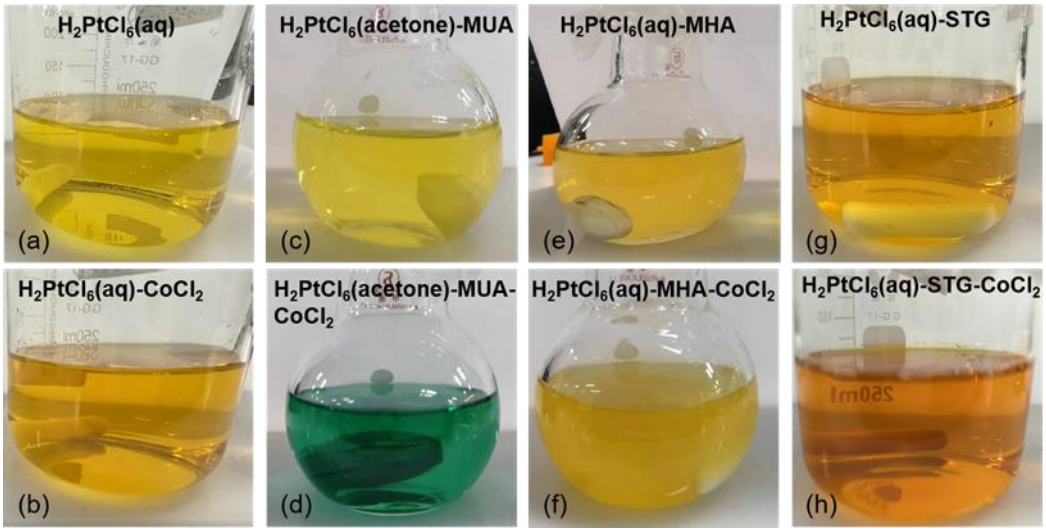

Supplementary Figure 8. Photographs of the solution color change after the addition of small molecule additives.

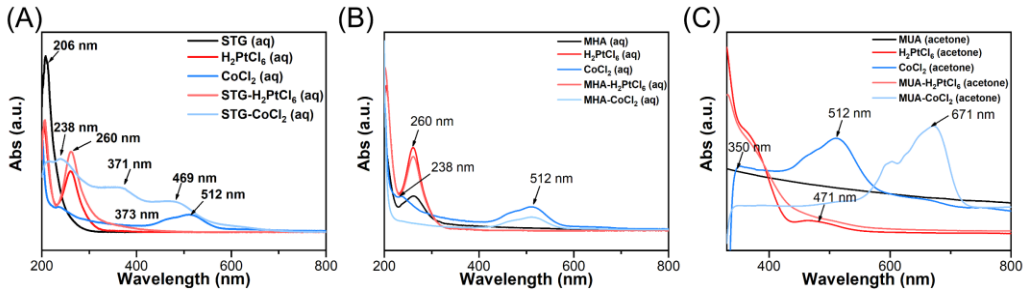

Supplementary Figure 9. UV–Vis spectra of (A) STG solution, H_2PtCl_6, and $CoCl_2$ solutions with and without STG, (B) MHA solution, H_2PtCl_6 and $CoCl_2$ solutions with and without MHA, (C) MUA acetone solution, H_2PtCl_6 and $CoCl_2$ acetone solutions with and without MUA.

In the UV-Vis spectrum of the H_2PtCl_6 aqueous solution (**Supplementary Figure 9A**), significant changes were observed in the absorption bands at 260 and 373 nm after STG was added. The absorption bands at 206 and 260 nm are attributed to ligand-to-metal charge transfer transitions, precisely corresponding to the $^1A_1g \rightarrow {}^1T_1u$ transition [1]. Additionally, the absorption band at 373 nm is assigned to *d-d* transitions, reflecting the octahedral symmetry of the $[PtCl_6]^{2-}$ configuration [2]. These results indicate that the sulfhydryl groups of STG replaced partial of the Cl liands and coordinated with

Pt (IV) [3]. Similarly, new absorption bands appeared at 238, 371, and 469 nm in the UV-Vis spectrum of the $CoCl_2$ solution with added STG, suggesting coordination between Co (II) and the carboxyl groups of STG [4]. Notably, when longer-chain additives MHA and MUA were added, the UV-Vis spectra of H_2PtCl_6 showed no significant changes, likely due to increased steric hindrance preventing the coordination between Pt (IV) and the sulfhydryl groups in the additives (**Supplementary Figure 9B-C**).

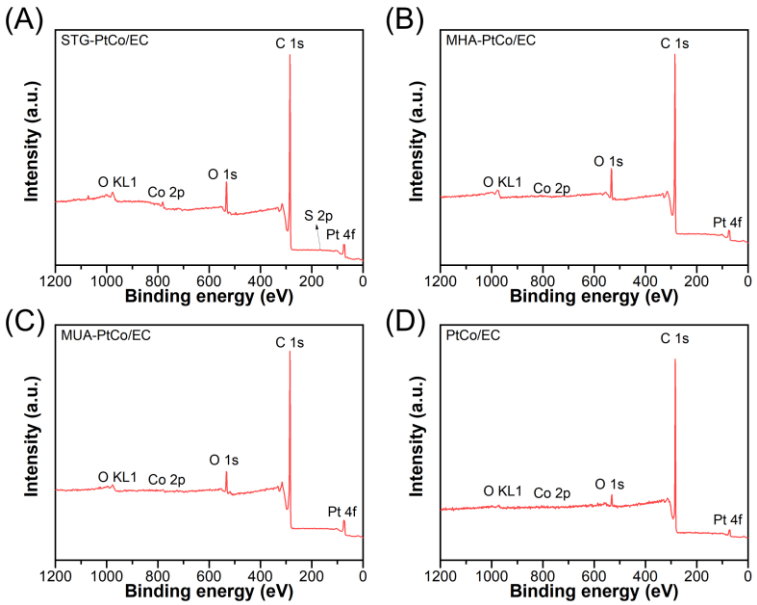

Supplementary Figure 10. XPS survey spectra of (A) STG-PtCo/EC, (B) MHA-PtCo/EC, (C) MUA-PtCo/EC and (D) PtCo/EC.

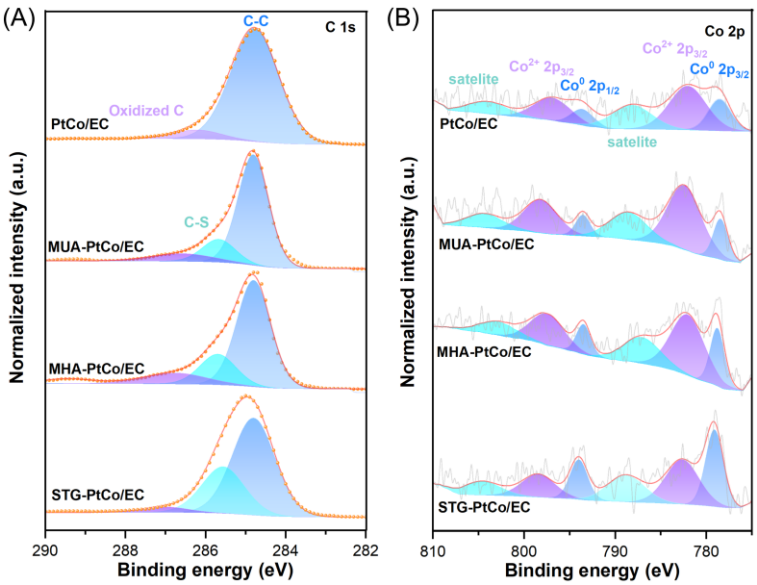

Supplementary Figure 11. (A) C 1s XPS spectra, (B) Co 2p XPS spectra of STG-PtCo/EC and the relevant samples.

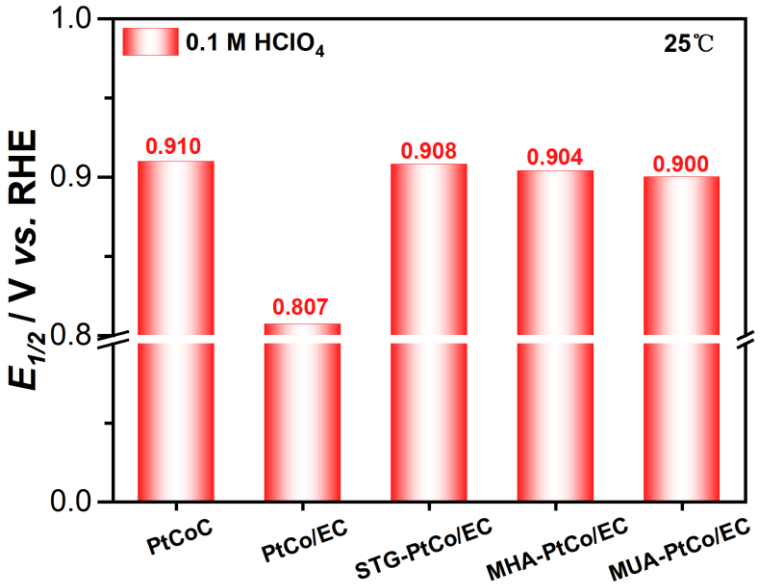

Supplementary Figure 12. $E_{1/2}$ in O_2-saturated 0.1 M $HClO_4$ at 25℃.

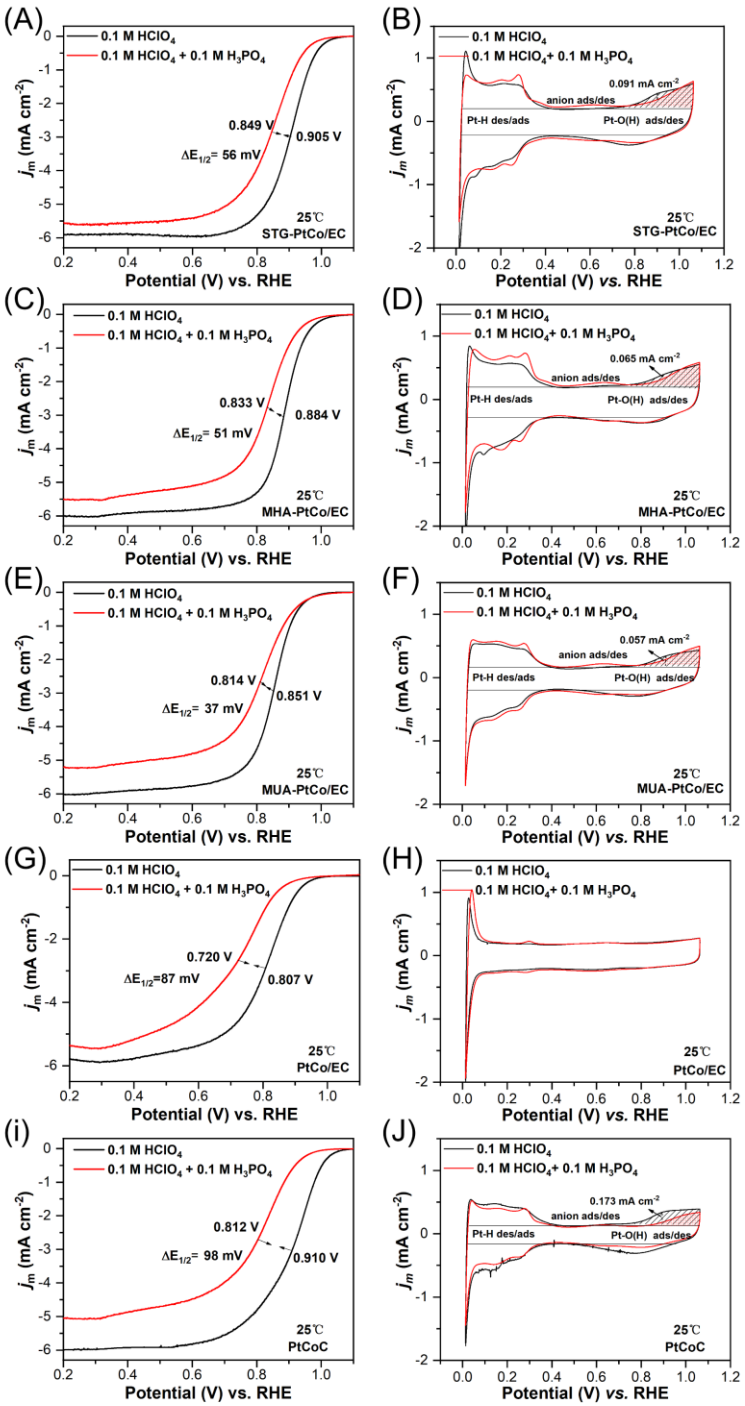

Supplementary Figure 13. LSV and CV curves of the as-synthesized catalysts in 0.1 M $HClO_4$ and 0.1 M $HClO_4$ + 0.1 M H_3PO_4 at 25℃ for (A, B) STG-PtCo/EC, (C, D) MHA-PtCo/EC, (E, F) MUA-PtCo/EC, (G, H) PtCo/EC, and (I, J) commercial PtCoC.

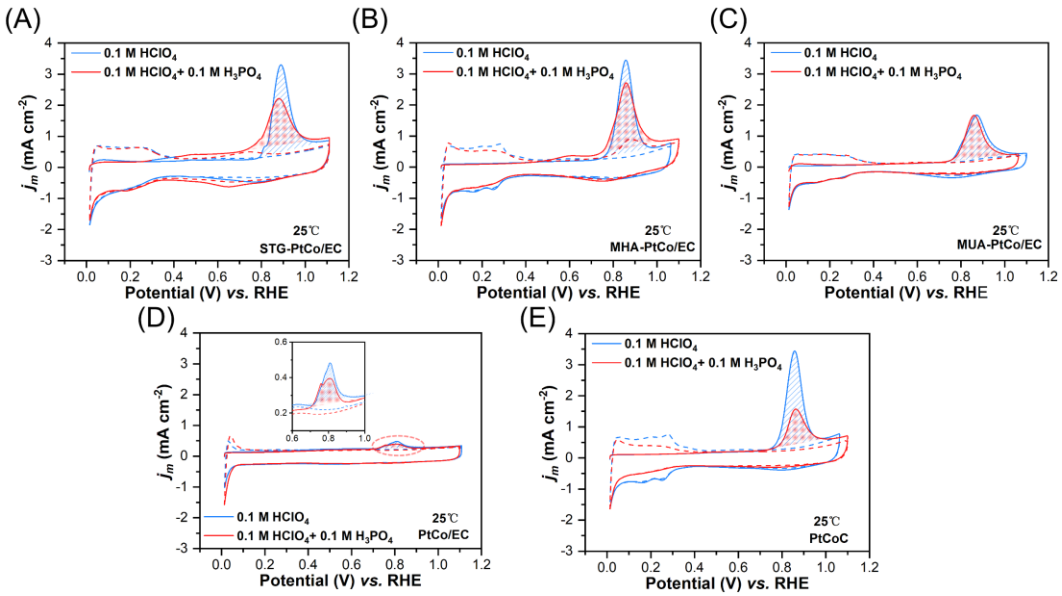

Supplementary Figure 14. CO stripping voltammograms of (A) STG-PtCo/EC, (B) MHA-PtCo/EC, (C) MUA-PtCo/EC, (D) PtCo/EC and (E) commercial PtCoC in 0.1 M $HClO_4$ and 0.1 M $HClO_4$ + 0.1 M H_3PO_4 at 25°C.

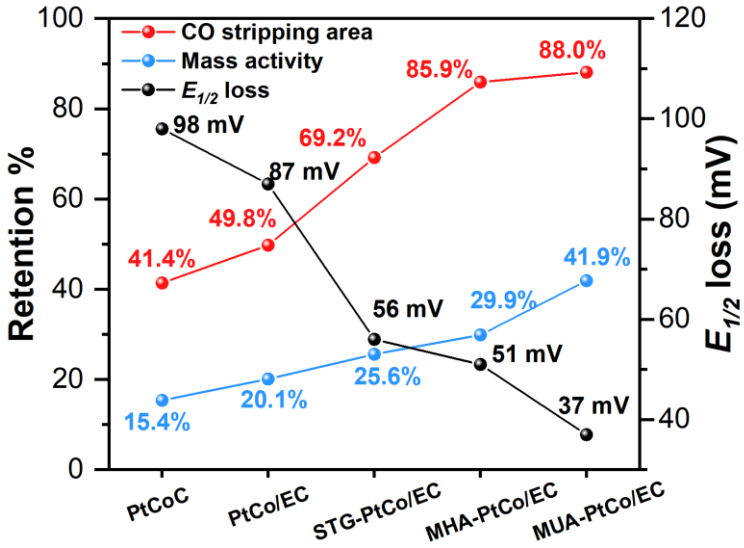

Supplementary Figure 15. Correlation of the $E_{1/2}$ decay values, CO-stripping area retention and MA retention of the corresponding electrocatalysts in 0.1 M $HClO_4$ and 0.1 M $HClO_4$ + 0.1 M H_3PO_4. Retention% = (value in 0.1 M $HClO_4$ + 0.1 M H_3PO_4/ value in 0.1 M $HClO_4$) × 100%.

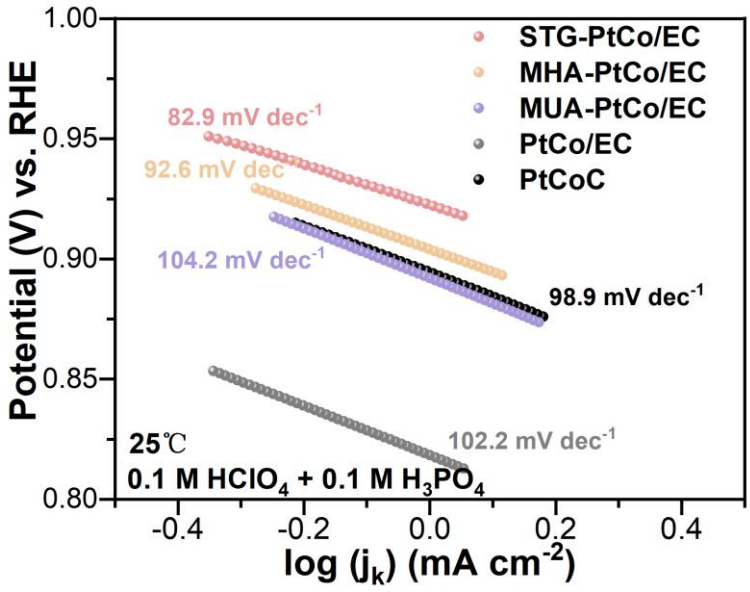

Supplementary Figure 16. Tafel Slopes in O_2-saturated 0.1 M $HClO_4$ + 0.1 M H_3PO_4 at 25℃.

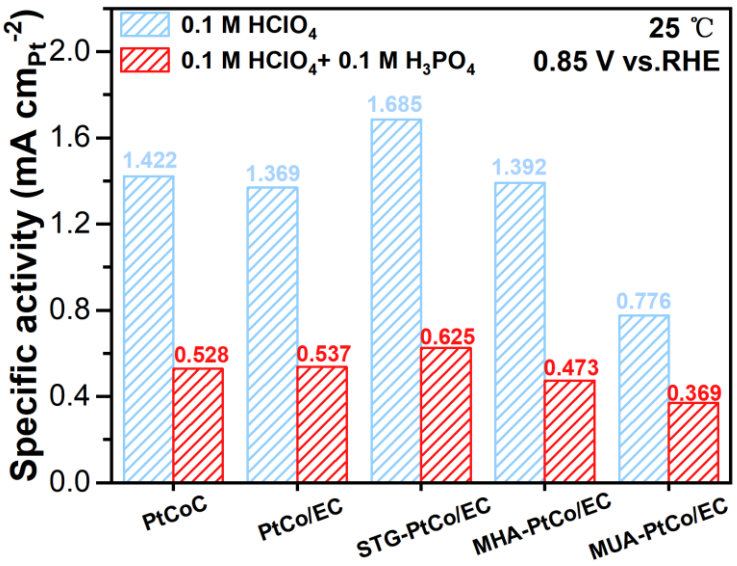

Supplementary Figure 17. Comparison of specific activity of ORR in 0.1 M $HClO_4$ and 0.1 M $HClO_4$ + 0.1 M H_3PO_4 at 25℃.

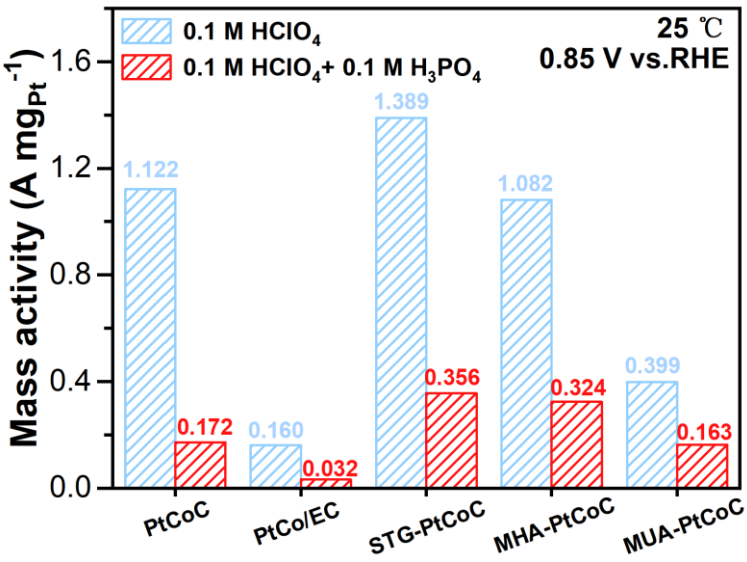

Supplementary Figure 18. Comparison of mass activity of ORR in 0.1 M $HClO_4$ and 0.1 M $HClO_4$ + 0.1 M H_3PO_4 at 25℃.

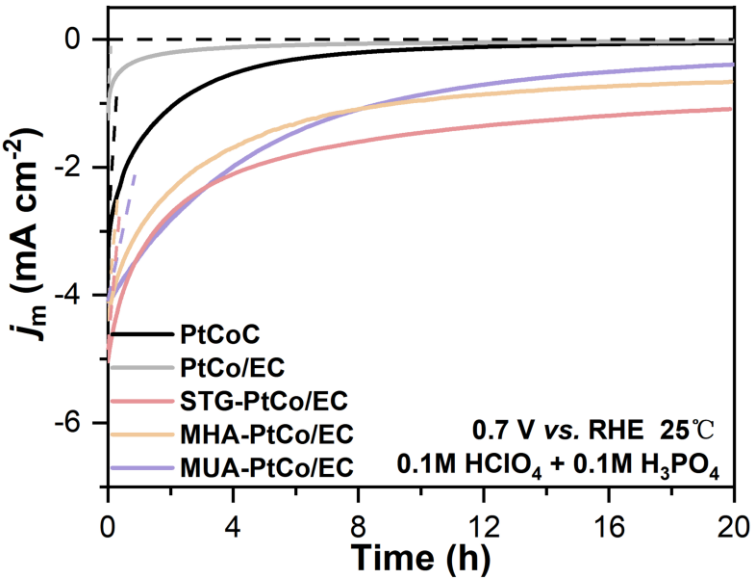

Supplementary Figure 19. The i-t curves at constant potentials of 0.7 V in 0.1 M $HClO_4$ + 0.1 M H_3PO_4 at 25℃.

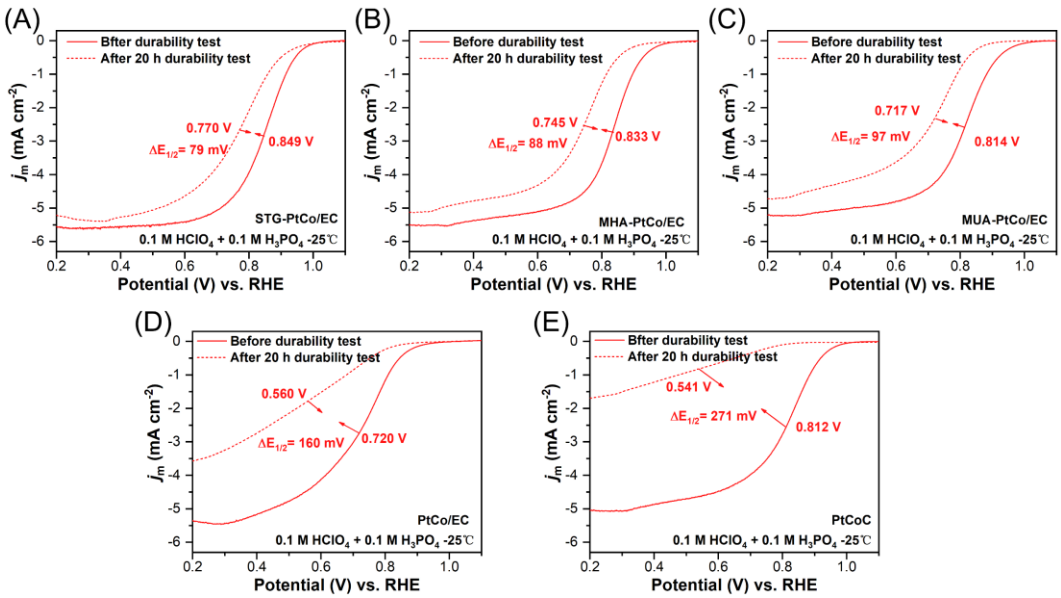

Supplementary Figure 20. ORR polarization curves of (A) STG-PtCo/EC, (B) MHA-PtCo/EC, (C) MUA-PtCo/EC, (D) PtCo/EC and (E) commercial PtCoC before and after the i-t tests in 0.1 M $HClO_4$ + 0.1 M H_3PO_4 at 25°C.

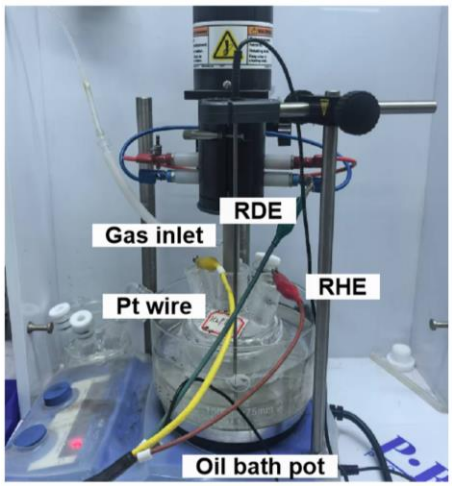

Supplementary Figure 21. Image of the HT-RDE equipment.

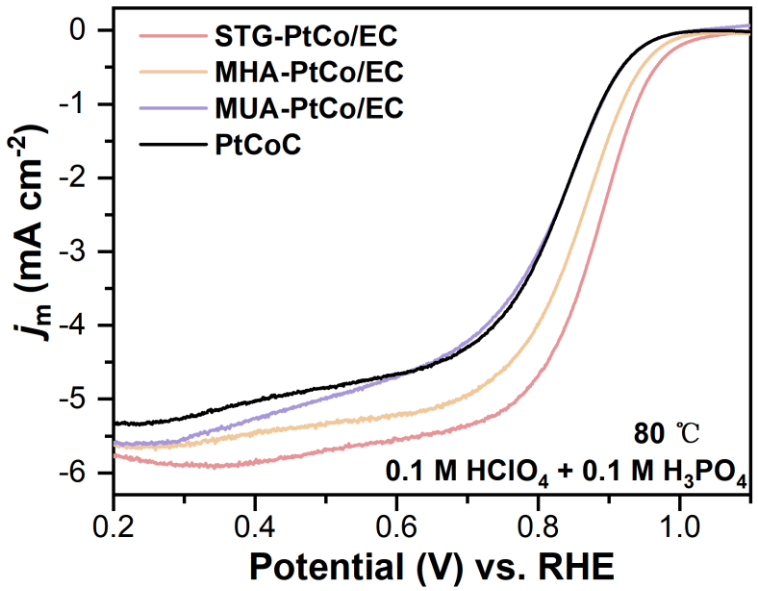

Supplementary Figure 22. ORR polarization curves of the synthesized catalysts and commercial PtCoC in O_2-saturated 0.1 M $HClO_4$ + 0.1 M H_3PO_4 at 80℃.

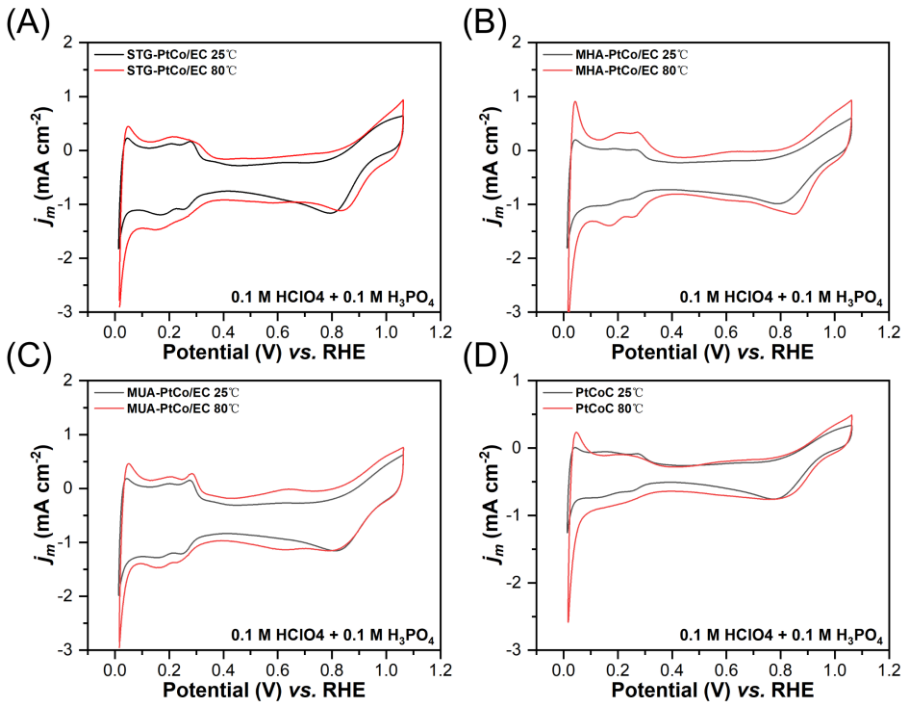

Supplementary Figure 23. CV curves comparison in 0.1 M $HClO_4$ + 0.1 M H_3PO_4 at 25℃ and 80℃ for (A) STG-PtCo/EC, (B) MHA-PtCo/EC, (C) MUA-PtCo/EC and (D) commercial PtCoC.

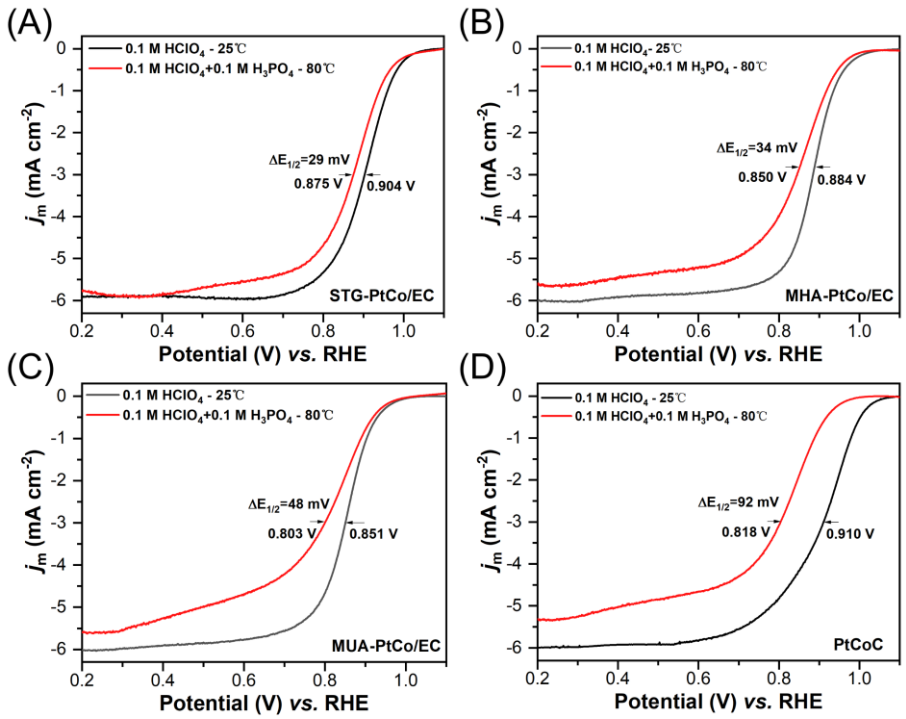

Supplementary Figure 24. ORR polarization curves comparison in 0.1 M $HClO_4$ at 25°C and 0.1 M $HClO_4$ + 0.1 M H_3PO_4 at 80°C for (A) STG-PtCo/EC, (B) MHA-PtCo/EC, (C) MUA-PtCo/EC and (D) commercial PtCoC.

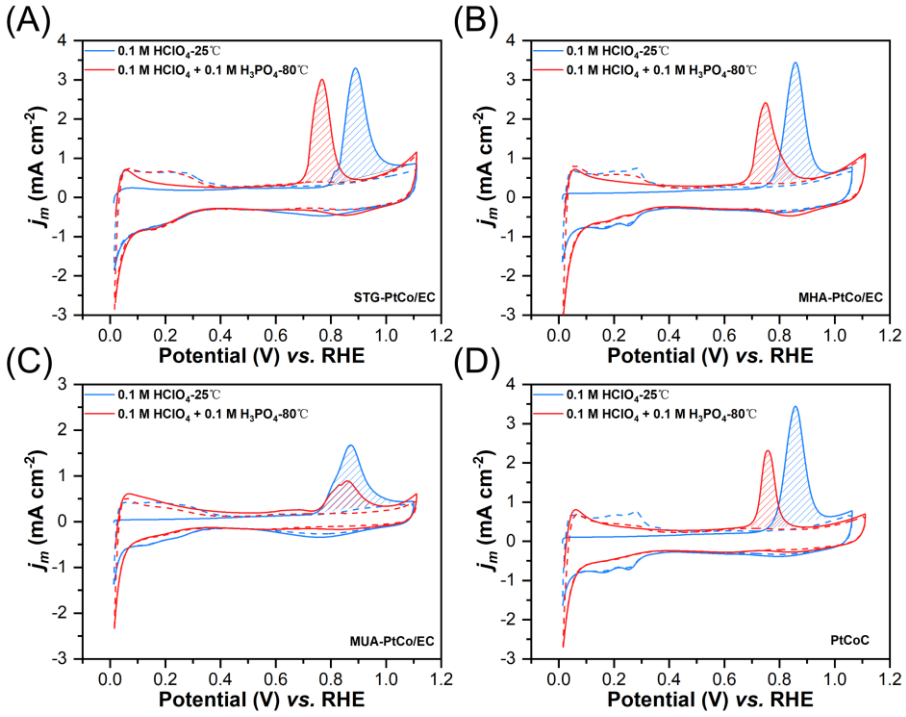

Supplementary Figure 25. CO stripping voltammograms comparison in 0.1 M $HClO_4$ at 25°C and 0.1 M $HClO_4$ + 0.1 M H_3PO_4 at 80°C for (A) STG-PtCo/EC, (B) MHA-PtCo/EC, (C) MUA-PtCo/EC and (D) commercial PtCoC.

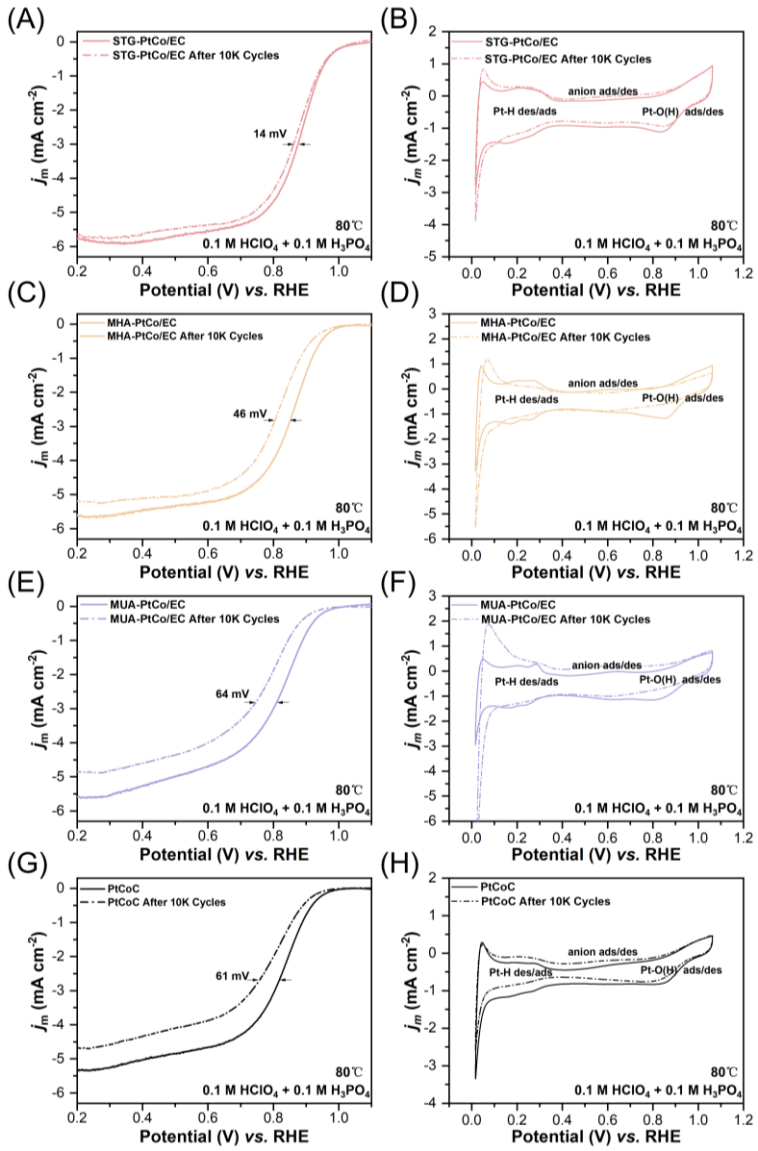

Supplementary Figure 26. LSV and CV curves of the as-synthesized catalysts before and after 10,000 ADT cycles in O_2-saturated 0.1 M $HClO_4$ + 0.1 M H_3PO_4 at 80°C for (A, B) STG-PtCo/EC, (C, D) MHA-PtCo/EC, (E, F) MUA-PtCo/EC and (G, H) commercial PtCoC.

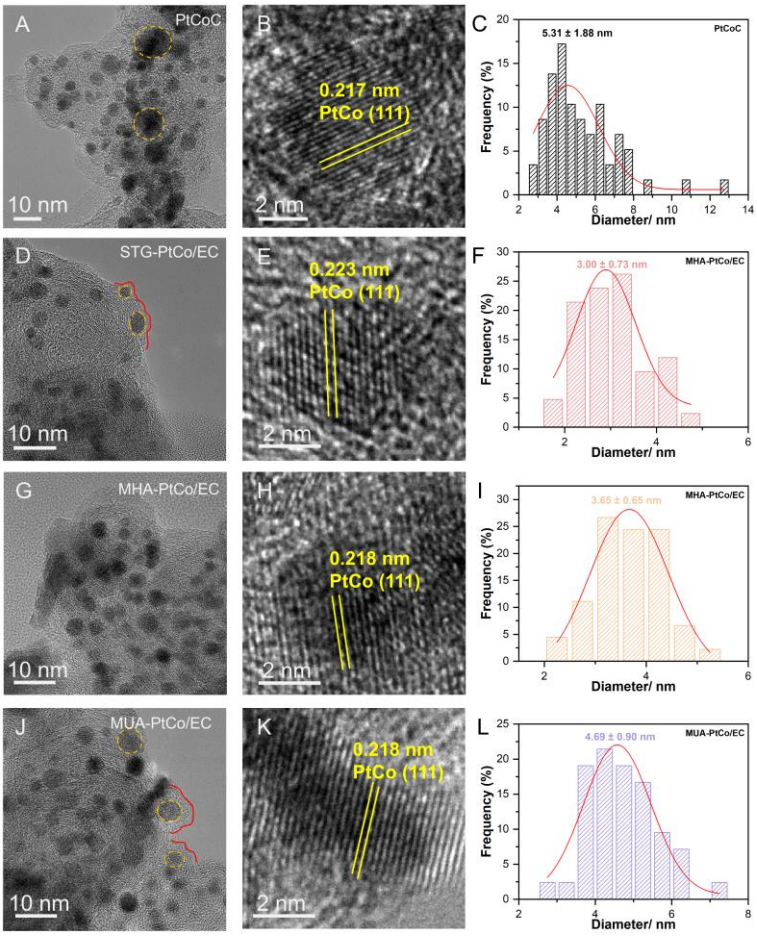

Supplementary Figure 27. TEM, HR-TEM images, and particle size distributions of (A-C) commercial PtCoC, (D-F) STG-PtCo/EC, (G-I) MHA-PtCo/EC, and (J-L) MUA-PtCo/EC after 10,000 potential cycles in 0.1 M $HClO_4$ + 0.1 M H_3PO_4 at 80 °C.

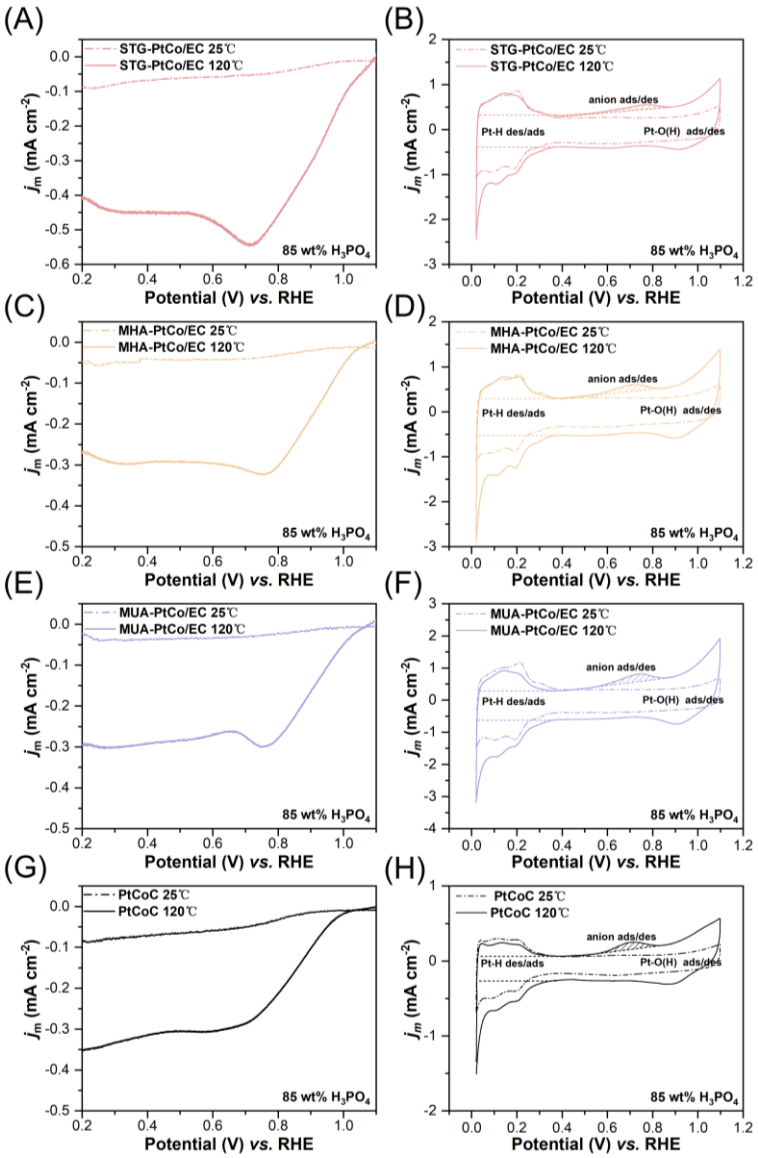

Supplementary Figure 28. LSV and CV curves of the as-synthesized catalysts in 85wt% H_3PO_4 at 25℃ and 120℃ for (A, B) STG-PtCo/EC, (C, D) MHA-PtCo/EC, (E, F) MUA-PtCo/EC and (G, H) commercial PtCoC.

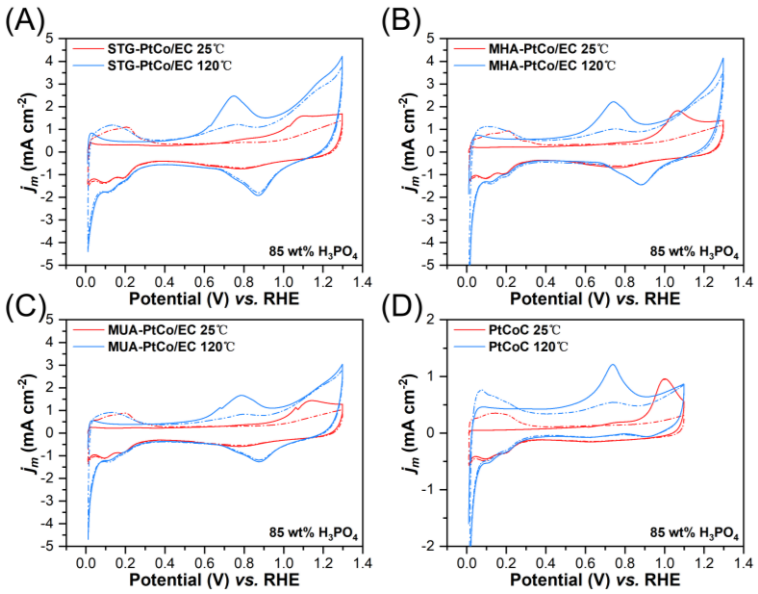

Supplementary Figure 29. CO stripping voltammograms comparison in 85 wt% H_3PO_4 at 25℃ and 120℃ for (A) STG-PtCo/EC, (B) MHA-PtCo/EC, (C) MUA-PtCo/EC and (D) commercial PtCoC.

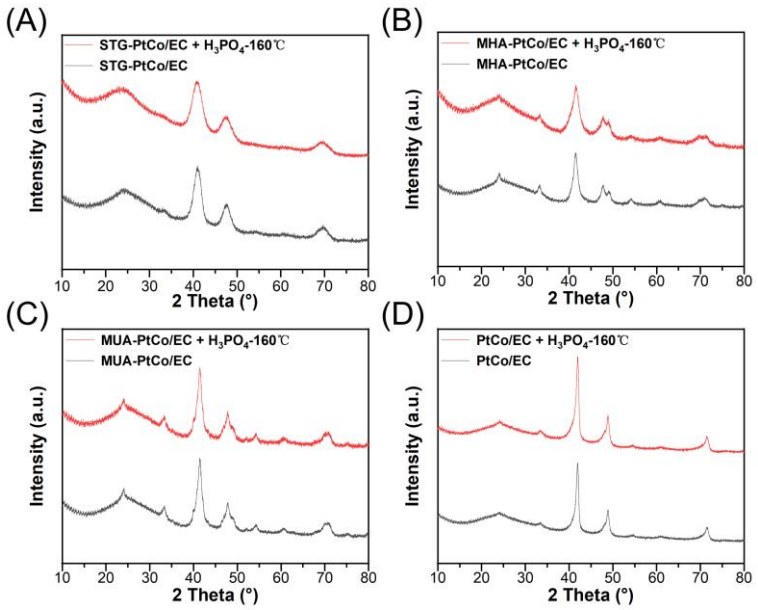

Supplementary Figure 30. XRD pattern of (A) STG-PtCo/EC, (B) MHA-PtCo/EC, (C) MUA-PtCo/EC and (D) PtCo/EC before and after treated with 85wt% H_3PO_4 at 160 °C for 18 h.

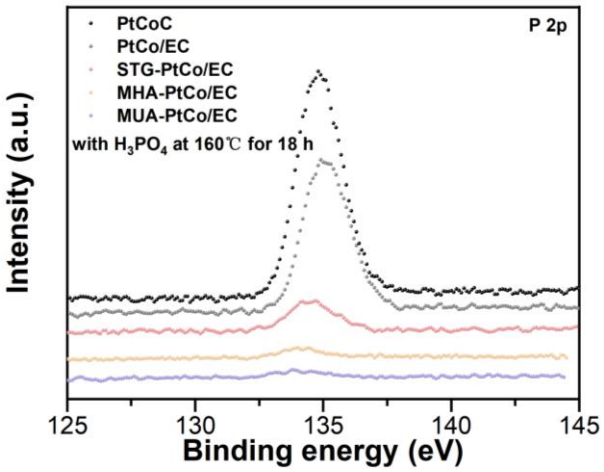

Supplementary Figure 31. XPS results of P 2p orbits of the as-synthesized electrocatalysts after treated with 85wt% H_3PO_4 at 160 °C for 18 h.

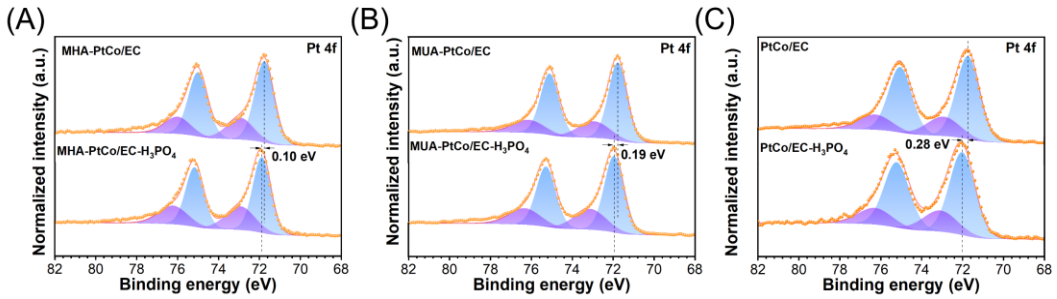

Supplementary Figure 32. XPS results of Pt 4f orbits of (A) MHA-PtCo/EC, (B) MUA-PtCo/EC and (C) PtCo/EC before and after treated with 85wt% H_3PO_4 at 160 °C for 18 h.

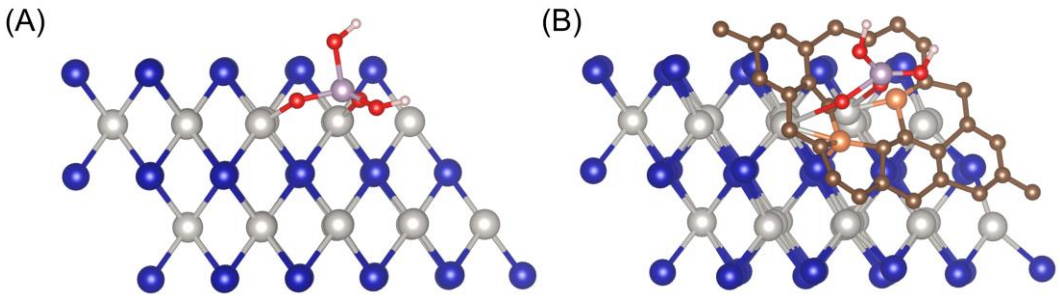

Supplementary Figure 33. Geometric structures of $H_2PO_4^-$ adsorption on PtCo (111) of (A) PtCo/EC and (B) STG-PtCo/EC. White, blue, orange, brown, purple, red, and pink balls represent Pt, Co, S, C, P, O, and H atoms, respectively.

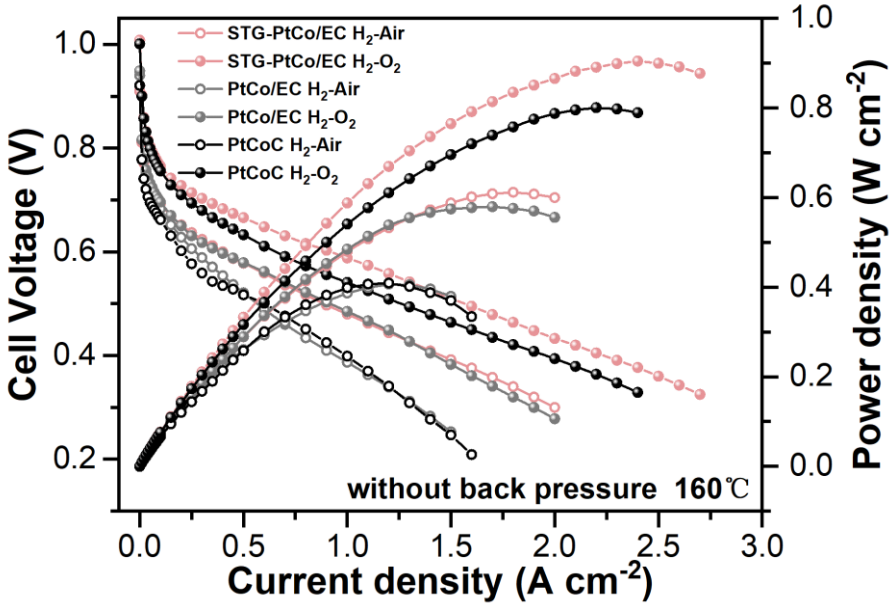

Supplementary Figure 34. H_2/air and H_2/O_2 fuel cell polarization and power density curves with low Pt loading (0.30 mg_{Pt} cm^{-2} in the cathode) at 160℃ without back-pressure.

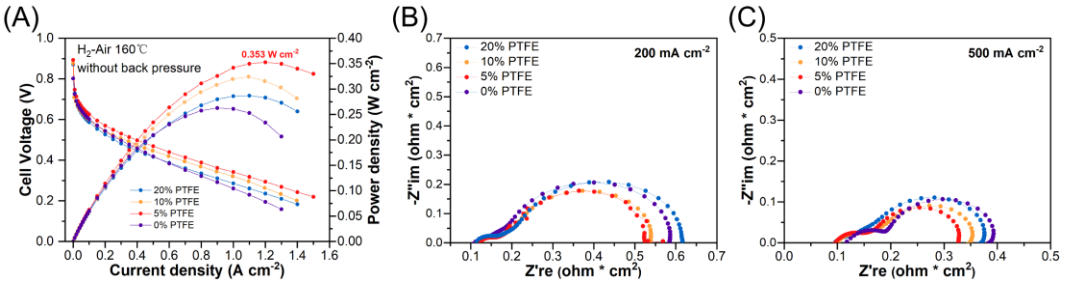

Supplementary Figure 35. (A) Polarization and power density curves of STG-PtCo/EC with ultra-low cathode Pt loading of 0.10 mg_{Pt} cm^{-2} with different PTFE binder content at 160℃ (H_2/air) without back-pressure. EIS spectra at constant current density of (B) 200 mA cm^{-2} and (C) 500 mA cm^{-2}.

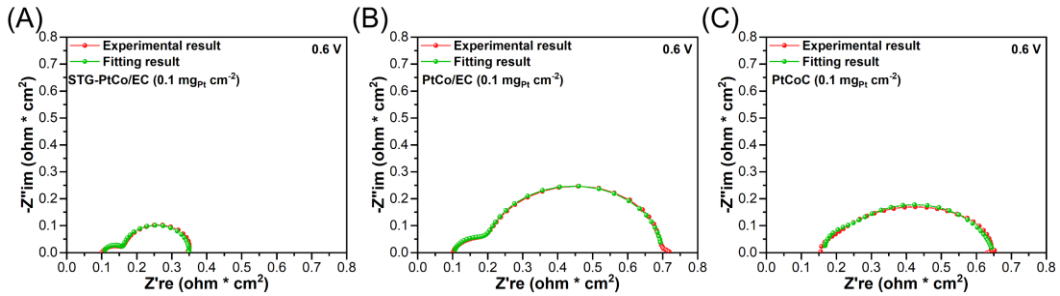

Supplementary Figure 36. Fitting results of the Nyquist plots of (A) STG-PtCo/EC, (B) PtCo/EC and (C) commercial PtCoC.

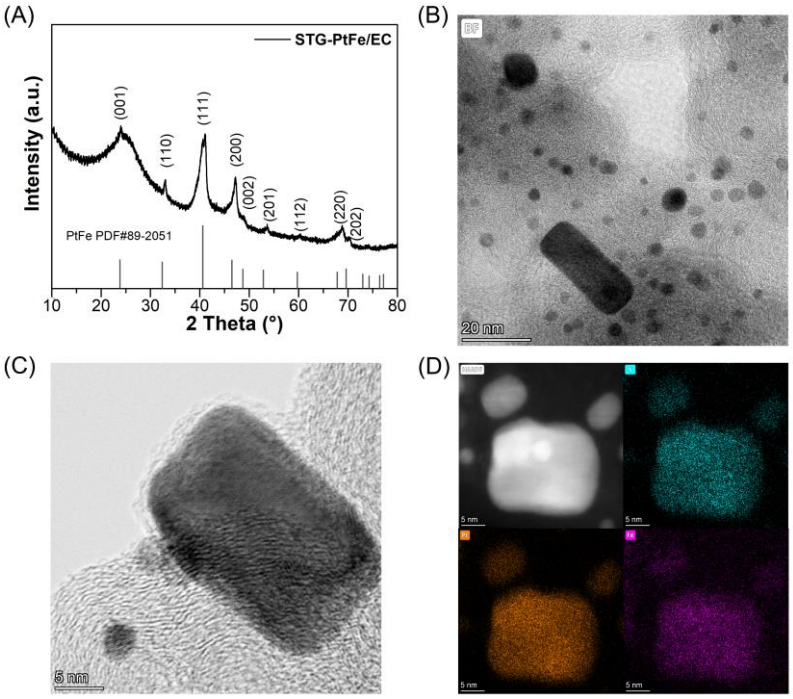

Supplementary Figure 37. (A) XRD pattern, (B-C) TEM images and (D) EDS mapping of STG-PtFe/EC.

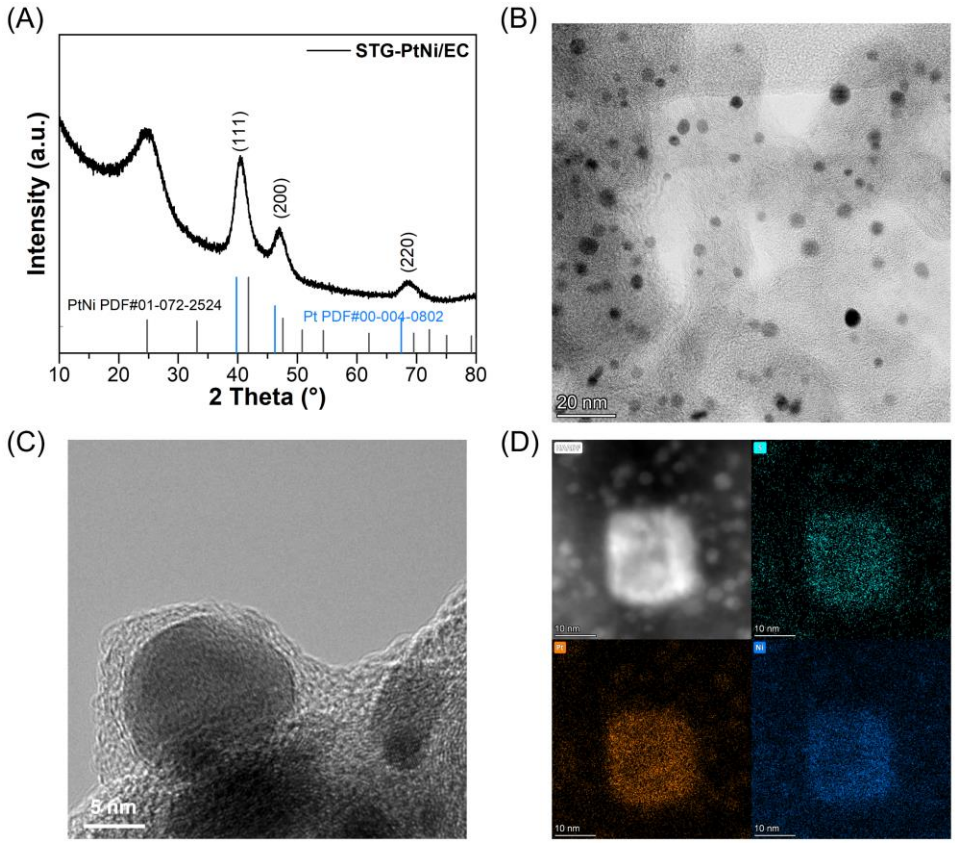

Supplementary Figure 38. (A) XRD pattern, (B-C) TEM images and (D) EDS mapping of STG-PtNi/EC.

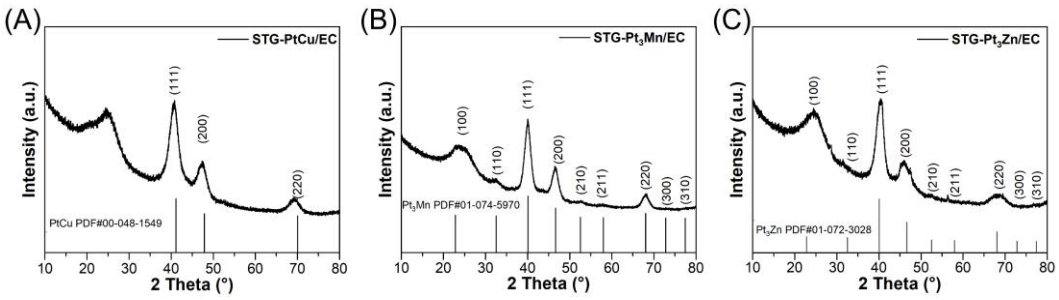

Supplementary Figure 39. XRD patterns of (A) STG-PtCu/EC, (B) STG-Pt_3Mn/EC and (C) STG-Pt_3Zn/EC.

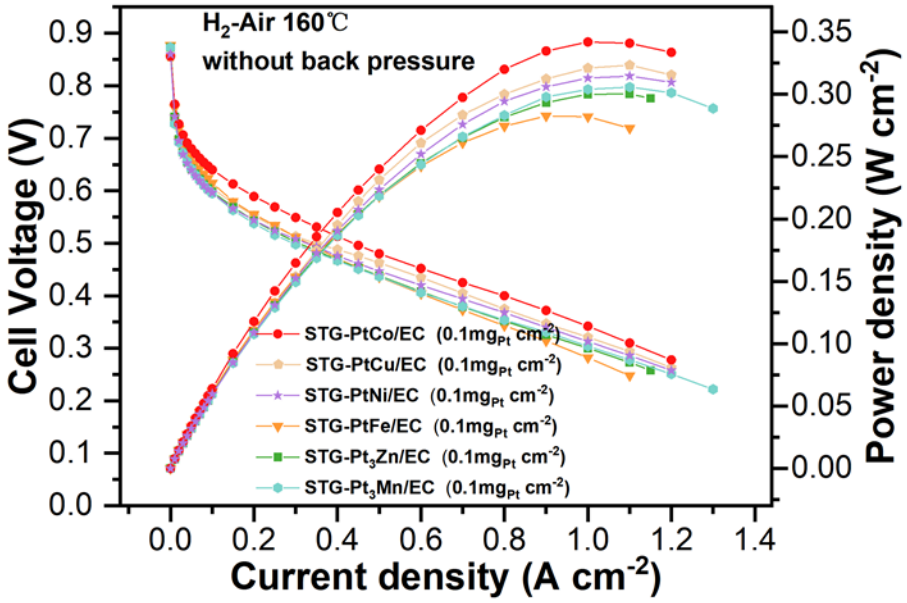

Supplementary Figure 40. Polarization and power density curves of different as-synthesized electrocatalysts with ultra-low Pt loading (0.10 mg_{Pt} cm^{-2} in the cathode) at 160℃ (H_2/air) without back-pressure.

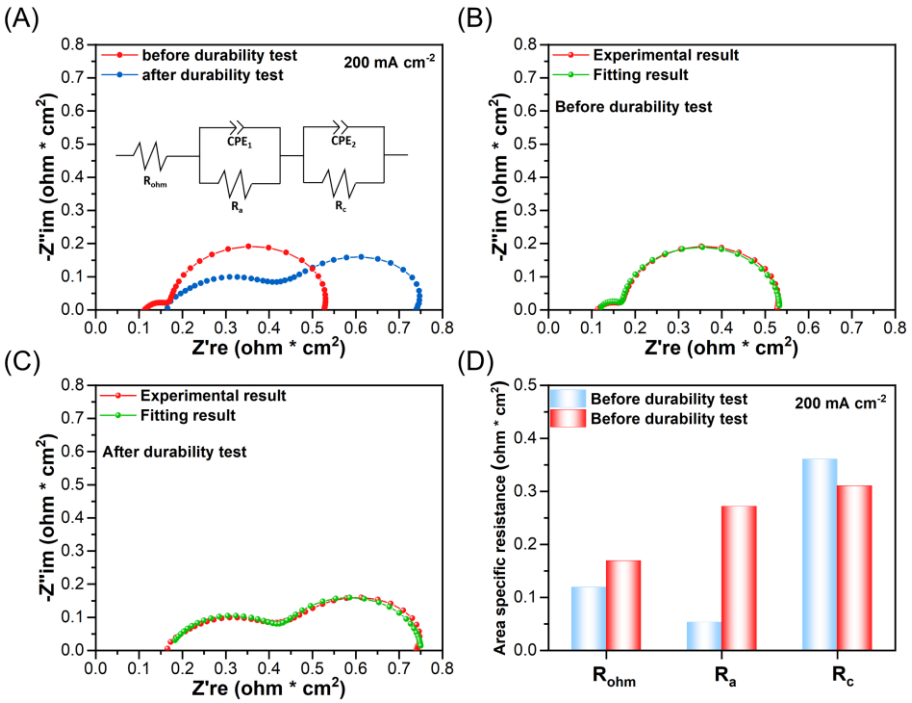

Supplementary Figure 41. EIS analysis of the MEA with STG-PtCo/EC as the anode (0.1 mg_{Pt} cm^{-2}) at a constant current density of 200 mA cm^{-2} before and after durability test. (A) Nyquist plots (inset: equivalent circuit). Fitting results of the Nyquist plots (B) before and (C) after durability test. (D) Fitted values of various impedances.

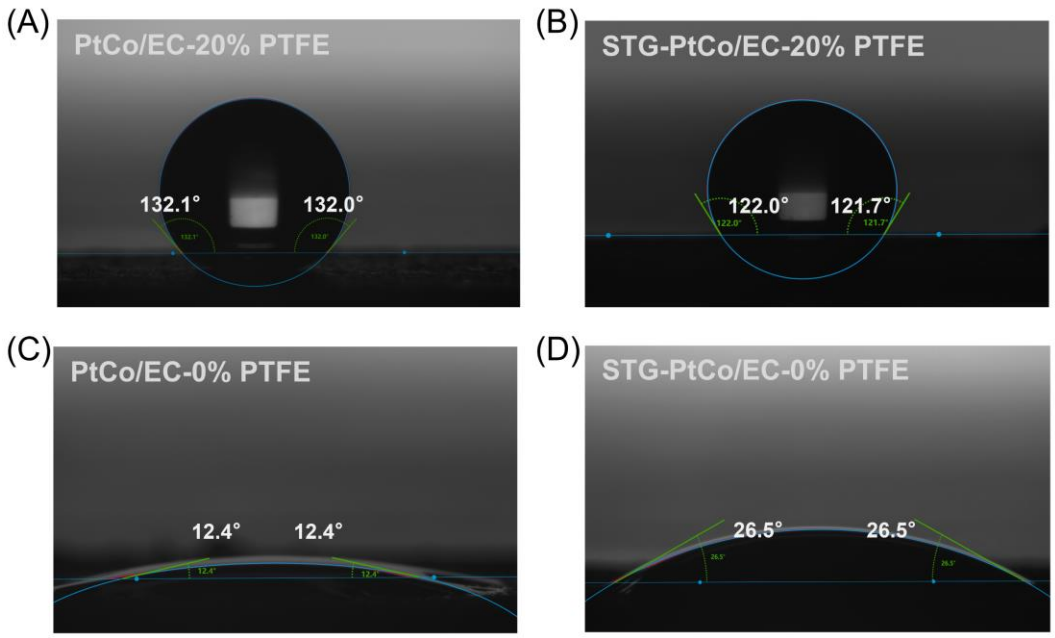

Supplementary Figure 42. Contact angle tests for PA on the cathode catalyst layers of (A) PtCo/EC with 20 % PTFE, (B) STG-PtCo/EC with 20 % PTFE, (C) PtCo/EC with 0 % PTFE and (D) STG-PtCo/EC with 0 % PTFE.

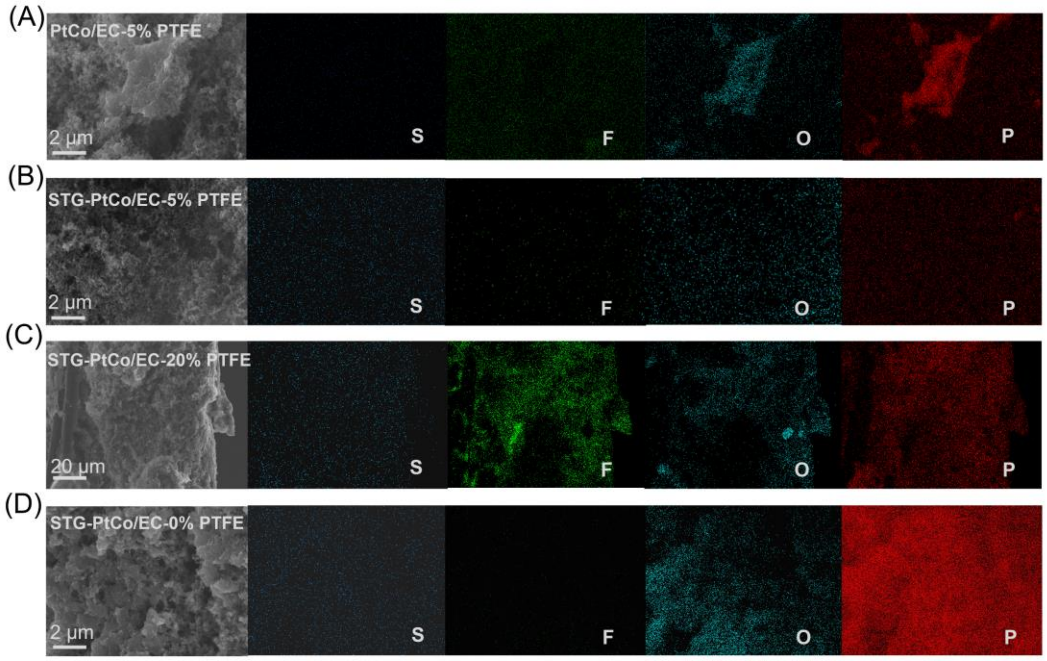

Supplementary Figure 43. EDS mapping of the cross-sections of the cathode catalyst layers of (A) PtCo/EC with 5 % PTFE, (B) STG-PtCo/EC with 5 % PTFE, (C) STG-PtCo/EC with 20 % PTFE and (D) STG-PtCo/EC with 0 % PTFE after HT-PEMFCs tests.

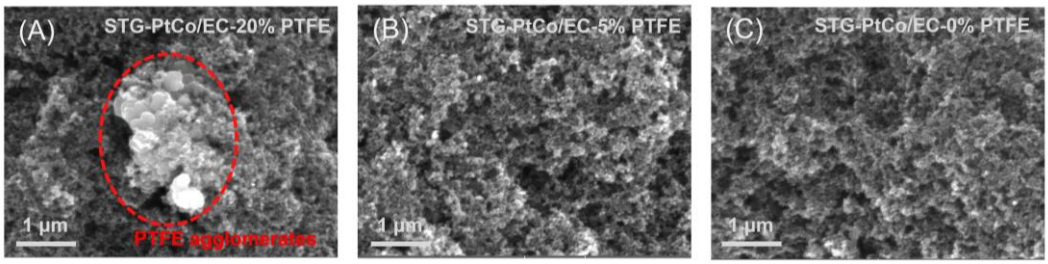

Supplementary Figure 44. SEM images of the microstructure of catalyst layers of (A) STG-PtCo/EC with 20% PTFE, (B) STG-PtCo/EC with 5% PTFE and (C) STG-PtCo/EC with 0% PTFE at a magnification of 50,000x.

Supplementary Table 1. The ICP-AES results of different samples.

Sample	Pt wt%	Co wt%
PtCo/EC	20.42	6.11
STG-PtCo/EC	21.08	6.20
MHA-PtCo/EC	20.77	5.91
MUA-PtCo/EC	21.92	6.03

Supplementary Table 2. Elemental analysis results of the additive-assisted PtCo/EC precursor powders and the final samples after high-temperature heat treatment.

Sample	C wt%	H wt%	N wt%	S wt%
H_2PtCl_6-$CoCl_2$/KB	17.74	2.033	0.1	0.465
PtCo/EC	66.77	0.748	0.11	0.576
STG-H_2PtCl_6-$CoCl_2$/KB	24.52	1.654	0.06	6.975
STG-PtCo/EC	59.12	0.819	0.07	2.508
MHA-H_2PtCl_6-$CoCl_2$/KB	24.95	2.617	0.09	7.173
MHA-PtCo/EC	62.23	0.558	0.13	2.302
MUA-H_2PtCl_6-$CoCl_2$/KB	30.48	3.489	0.07	6.619
MUA-PtCo/EC	64.91	0.837	0.15	2.042

Supplementary Table 3. The ratio of Co^0 to Co^{2+} content in the Co 2p XPS spectra.

Sample	Area ratio of Co^{2+} 2p $_{3/2}$	Area ratio of Co^0 2p $_{3/2}$	Co^0/Co^{2+}
PtCo/EC	1.00	0.43	0.43
MUA-PtCo/EC	1.00	0.27	0.27
MHA-PtCo/EC	1.00	0.40	0.40
STG-PtCo/EC	1.00	0.91	0.91

Supplementary Table 4. The ICP-AES results of different STG-PtM/EC samples.

Sample	Pt wt%	M wt%
STG-PtFe/EC	22.41	6.23
STG-PtNi/EC	20.18	5.77
STG-PtCu/EC	21.96	6.85
STG-Pt_3Mn/EC	19.88	2.06
STG-Pt_3Zn/EC	20.10	2.24

References

1. Swihart D. L., Mason W. R.; Electronic spectra of octahedral platinum (IV) complexes, *Inorganic Chemistry* **1970,** *9*, 1749-1757; DOI: 10.1021/ic50089a029.
2. Shelimov B., Lambert J.-F., Che M., Didillon B.; Initial Steps of the Alumina-Supported Platinum Catalyst Preparation: A Molecular Study by 195Pt NMR, UV–Visible, EXAFS, and Raman Spectroscopy, *Journal of Catalysis* **1999,** *185*, 462-478; DOI: 10.1006/jcat.1999.2527.
3. Gomez S., Erades L., Philippot K., Chaudret B., Collière V., Balmes O., Bovin J.-O.; Platinum colloids stabilized by bifunctional ligands : self-organization and connection to gold, *Chemical Communications* **2001,** 1474-1475; DOI: 10.1039/B103781C.
4. Song T. W., Xu C., Sheng Z. T., Yan H. K., Tong L., Liu J., Zeng W. J., Zuo L. J., Yin P., Zuo M., Chu S. Q., Chen P., Liang H. W.; Small molecule-assisted synthesis of carbon supported platinum intermetallic fuel cell catalysts, *Nat. Commun.* **2022,** *13*, 6521; DOI: 10.1038/s41467-022-34037-7.